Identification of Key Genes Related to Immune Infiltration of Cirrhosis via Bioinformatics Analysis

Tong-Yue Du
Nanjing Hospital, Nanjing University of Chinese Medicine
Yi-Shan Zheng (doctor0219@163.com)
Nanjing Hospital, Nanjing University of Chinese Medicine

Research Article

Keywords: Cirrhosis, Bioinformatic analysis, immune infiltration, CIBERSORT, Pathway

Posted Date: January 3rd, 2022

DOI: https://doi.org/10.21203/rs.3.rs-1054780/v1

Abstract

Background

Accumulating researches have indicated that cirrhosis is a vital risk factor for morbidity and mortality worldwide. Nevertheless, the underlying immune-related molecular mechanism remains indistinct.

Methods

Gene expression profiles of GSE89377 and GSE139602 were investigated to identify differentially expressed genes (DEGs) related to cirrhosis. Enrichment analysis for DEGs was explored. CIBERSORT algorithm was used for evaluating DEGs immune infiltration. The String and Cytoscape database were utilized for analyses hub DEGs with a high tight connection, and the association between hub DEGs and immune cells infiltration was analyzed by Spearman method. Finally, the underlying molecular mechanism of the key DEGs was predicted via KEGG pathway analysis.

Results

In all, 299 DEGs were attained among them 136 and 163 were up and down-regulated respectively. Then Enrichment function of DEGs and CIBERSORT algorithm showed that they are significant in immune and inflammatory responses. Four hub DEGs (*ACTB, TAGLN, VIM, SOX9*) were identified. Subsequently, the immune infiltration findings indicated that, the hub DEGs highly related immune cells. Finally, KEGGs pathways were predicted related with *ACTB*.

Conclusions

This study revealed key DEGs may implement inflammatory immune responses with cirrhosis, which could be used as biomarkers or therapeutic targets.

1. Introduction

Cirrhosis is growing common reason of morbidity and mortality, with an annual incidence of 15.33-132.6 per 100000 people and approximately 1.03 million deaths per year worldwide[1-3]. Accumulating studies have revealed that cirrhosis was involved in multiple mechanisms, mainly including immune infiltration, necroinflammation and fibrogenesis. However, the underlying molecular mechanism, especially immune-related mechanism, remains unclear. Therefore, identification of key genes of immune infiltration in cirrhosis had been a hotspot in liver disease research field.

Microarrays and bioinformatics methodologies have been extensively used for screening variations of genetic at the genome sequencing[4, 5]. In our study, Two gene expression profiles of GSE89377 and GSE139602 derived from Gene Expression Omnibus (GEO) were analyzed. Then, we observed the infiltration condition of various immune cells in cirrhosis via CIBERSORT[6] algorithm. Subsequently, we performed the functional enrichment analysis of the DEGs based on Gene Ontology (GO) and the Kyoto Encyclopedia of Genes and Genomes (KEGG) database and detected hub DEGs with a high degree of connectivity. Finally, we performed the correlation within hub DEGs and immune cells, and KEGGs pathways were predicted for hub DEGs.

2. Material And Methods

The profile of genes related to cirrhosis were acquired from the GEO (http://www.ncbi. nlm.nih.gov/geo)[7], the GSE89377 series contained 13 normal liver tissue specimens and 12 cirrhosis tissue specimens which based on the GPL16947 platform Illumina HumanHT-12 V3.0 expression biochip, the GSE139602 series contained 6 normal liver tissue specimens and 20 cirrhosis tissue specimens, which based on the GPL13667 platform [HG-U219] Affymetrix Human Genome U219 array. Depending to the annotation information of platform were transformed the probe to the equivalent gene symbols.

2.2 Identification of DEGs in normal liver and cirrhosis

GEO2R is an interactive network instrument datasets in the GEO series to screen DEGs(https://www.ncbi.nlm.nih.gov/geo/geo2r/)[8]. In our study, GEO2R was used for identifying DEGs between normal liver and cirrhosis specimens. Genes without matching gene symbol, and genes with multiple probes were separately omitted and $|\mathrm{Log_2FC}| > 0.5$ adjusted $P < 0.05$ are the threshold standard for statistical significance. For the next step, the Venn Diagram with the R package (RRID: SCR_010943) was applied to detect the intersection DEGs among two datasets[9]. Meanwhile, heat maps and volcano maps of cirrhosis-related DEGs were created by the “ggplot2” packages.

2.3 Functional enrichment analyses of the cirrhosis-related DEGs

GO analysis could annotate multiple functions of a set of genes, including cellular components (CCs), molecular functions (MFs), and biological processes (BPs). KEGG is a primary resource for us to obtain genetic biological functions and advanced genomic information[10]. KEGG signaling pathway analysis can suggest the biological pathways of specific disease-related genes and drugs. In present study, GO enrichment analysis and KEGG signal pathway analysis of the cirrhosis-related DEGs via cluster profiler package in R.

2.4 Immune cell infiltration related DEGs

We assessed immune cell infiltration of cirrhosis through the CIBERSORT algorithm[11]. CIBERSORT uses preprocessed gene expression profiles to speculate the cell composition of complex tissues. The LM22 gene file was used for defining 22 immune cell subcategories and analyses cirrhosis data, which were attained from the CIBERSORT web portal (http://CIBERSORT.stanford.edu/). The result was then directly combined and generated an entire matrix of immune cell fractions. The CIBERSORT results was visualized with the R packages (“Complex heatmap”, “ggpubr” and “ggplot2”)[12].

2.5 Construct protein and protein interaction (PPI) network and identify hub DEGs

The key DEGs and gene modules in cirrhosis can be identified via the PPI. First, cirrhosis-related DEGs were imported into the STRING online analysis software to predict the interaction between the proteins encoded by these genes(http://string-db.org/). Subsequently, on the basis of the STRING analysis, the Cytoscape software platform was used for constructing a PPI network of these genes, and the 4 optimal hub-DEGs with the highest related were screened by five methods (EPC, Degree, MNC, MCC and MCODE).

2.6 Correlation analyses between hub DEGs and infiltrating immune cells

We used CIBERSORT algorithm to identify and analyze previously obtained the immune-related genes, and obtain the expression of 22 types of immune cells[6]. Then, we used Spearman correlation analysis to probe the potential relations between the key DEGs and infiltrating immune cells with R software, and then the package of “ggpubr” was used to visualize the results.

2.7 Predicted Pathways associated with ten hub DEGs of cirrhosis

We accomplished KEGG pathway explore of genes associated with DEGs with “cluster Profiler” package in R, and drawn resulting pathway plot via “Pathview” package in R. The relevant locations of matching genes in the pathway were shown in red.

3. Results

3.1 Identify DEGs between and normal liver tissue and Cirrhosis tissue

In this study, the data set GSE89377 contains 13 normal liver samples and 12 cirrhosis samples, and a total of 723 cirrhosis-related DEGs were confirmed in cirrhosis tissue, including 270 down-regulated genes and 453 up-regulated genes. Volcano plots of GSE89377 are displayed in **Figure 1A**. The data set GSE139602 contains 6 normal liver samples and 20 cirrhosis samples, and a total of 3708 cirrhosis-related DEGs were confirmed in cirrhosis tissue compared with healthy patients, including 2576 down-regulated genes and 1132 up-regulated genes. Volcano plots of GSE139602 are displayed in **Figure 1B**.

3.2 Screening the cirrhosis-related DEGs

A total of 299 cirrhosis-related genes were screen out by overlapping DEGs, genes in GSE89377 and GSE139602 listed in **Table 1.** The co-expression of DEGs were displayed using a Venn diagram in **Figure 1C.** Then heat maps of the DEGs expression in the two samples are shown in **Figure 1D and Figure 1E** respectively**.**

3.3 Functional enrichment analyses

In this study, function enrichment analysis of these DEGs based on GO and KEGG database had to be carried out. As showed in **Figure 2A**, enriched biological processes (BPs) were mainly involved in the astrocyte differentiation, dendritic cell apoptotic process, establishment of lymphocyte polarity, immunological synapse formation and negative regulation of macrophage derived foam cell differentiation. The cellular components (CCs) were primarily enriched in collagen-containing extracellular matrix, basement membrane, blood microparticle, collagen trimer and microfibril. Enriched molecular functions (MFs) were mostly involved in external matrix structural constituent, G protein-coupled receptor binding, transmembrane receptor protein kinase activity, platelet-derived growth factor binding and dipeptidase activity. KEGG pathway explore displayed that Viral protein interaction with cytokine and cytokine receptor, Tight junction, cell adhesion molecules, leukocyte transendothelial migration, PI3K-Akt signaling pathway, Phagosome, Hepatitis C, ECM-receptor interaction, Complement and coagulation cascades and ABC transporters in **Figure 2B**.

3.4 Composition of infiltrating immune cells between normal liver and cirrhosis tissue.

Based on CIBERSORT algorithm investigated the top five immune cells (Monocytes-M0, Monocytes-M1, T-cell-CD4-memory-activated, T-cells-regulatory-Trags and T-cell-CD4-resting) expressed within all the tissues in **Figure 3A**. Then difference between healthy liver tissues and cirrhosis in immune infiltration with 22 subgroups of immune cells in **Figure 3B.** Finally, the significant variance of 11 kinds of immune cells between 19 normal patients and 32 cirrhosis patients was illustrated in **Figure 3C**.

3.5 Construct PPI network and identify hub DEGs

Cirrhosis-related co-expressed DEGs were imported into the STRING online analysis software. Then, the Cytoscape software platform was used for constructing a PPI network of these genes **(Figure 4A)**. Meanwhile, all DEGs with the highest connectivity were selected by EPC, Degree, MNC, MCC and MCOD methods and displayed in **Figure 4B-F**. Subsequently, four hub genes were obtained by intersection of the top ten Hub DEGs extracted by the five methods, as shown in **Figure 4G**. Finally, the variance was displayed between cirrhosis and normal tissues within two databases in **Figure 5A-D**.

3.6 Relation analyses between hub DEGs and immune cells

The results of the related investigation discovered that *ACTB* was positively related with B cell activated (r=0.83, *P*=5.71E-08), Type 17 T helper cell (r=0.83, *P*=1.51E-07), Macrophage (r=0.58, *P*=7.16E-06), Mast cell (r=0.80, *P*=1.51E-07), Effector memeoryCD8 T-cell(r=0.67, *P*=4.62E-14) and significantly negatively correlated with CD56dim natural killer cell (r=-0.67, *P*=5.71E-08), T helper cell of Type 1 (r=-0.66, *P*=1.51E-07), T helper cell of Type 2 (r=-0.89, *P*=0) (**Figure 6A**).

TAGLN was positively correlated with Central memory CD4 T cell (r=0.69, *P*=2.04E-08), Monocyte (r=0.58, *P*=9.30E-06) and correlated negatively with Eosinophil (r=-0.56, *P*=2.25E-05), Macrophage (r=-0.71, *P*=7.49E-09), T-cell regulatory (r=-0.74, *P*=3.95E-10), Natural killer T cell (r=-0.51, *P*=0.00), T helper cell

of Type 17 (r=-0.73, *P*=9.22E-10) (**Figure 6B**).

VIM was positively related with B cell activated (r=0.78, *P*=1.38E-11), Effector memory CD8 T-cell (r=0.53, *P*=5.69E-05), Mast cell (r=0.78, *P*=1.46E-11) and correlated negatively with T helper cell of Type 1 (r=-0.73, *P*=5.78E-10), T helper cell of Type 2 (r=-0.78, *P*=1.78E-11) (**Figure 6C**).

SOX9 was positively correlated with B cell activated (r=0.80, *P*=1.10E-12), Effector memory CD8 T cell (r=0.68, *P*=3.94E-08), Mast cell (r=0.81, *P*=1.01E-12), helper cell of Type 17 T (r=0.81, *P*=9.42E-13) and correlated negatively with natural killer cell CD56dim (r=-0.70, *P*<8.02E-09), T helper cell of Type 1 (r=-0.74, *P*=4.06E-10), T helper cell of Type 2 (r=-0.90, *P*= 0) (**Figure 6D**).

3.7 Predicted hub-DEGs-related Pathways of the Changes in cirrhosis

KEGG analysis can identify the pathways associated with the hub-DEGs alterations and frequently altered functions of neighbor genes. Total 39 pathways connected with hub DEGs for cirrhosis were screened using KEGG analysis (**Figure 2B)**. Importantly, hsa04145: Phagosome (**Figures 7; Table 2)**.

4. Discussion

Cirrhosis is one of most common liver diseases caused by alcoholic liver disease, chronic viral hepatitis, non-alcoholic fatty liver disease or non-alcoholic steatohepatitis, and other causes [13] [14]. To date, despite the various treatment for cirrhosis, including dietary control, drug therapy, and surgical intervention[15], challenges still remain with modest treatment effect, high adverse effect and high risk of liver function deterioration. Therefore, screening promising diagnosis and therapy biomarkers for the cirrhosis is urgently needed for preventing to develop the end-stage of the cirrhosis. Recently, increasing evidence had revealed that the pathogenesis of cirrhosis may be associated with immune and inflammatory responses[16, 17]. Interestingly, increasing studies had showed inhibition of inflammatory cytokines was expected to be a promising therapy for cirrhosis by inhibiting the accumulation of extracellular matrix[16-18]. In this study, we identified immune relevant genes and deeper explore the effect of immune cell infiltration in cirrhosis using bioinformatics analysis.

First, total of 299 DEGs were screened out as candidate biomarkers. We identified the underlying mechanism of DEGs by enrichment function. GO enrichment explore indicated that DEGs were markedly correlated with were mainly involved in the astrocyte differentiation, dendritic cell apoptotic process, establishment of lymphocyte polarity, immunological synapse formation and negative regulation of macrophage derived foam cell differentiation. Further, these genes were involved in leukocyte transendothelial migration, Complement and coagulation cascades, and other pathways via the KEGG analysis.

Then, based on the above analysis, CIBERSORT algorithm was used to analyze the immune differences between normal and cirrhotic tissues. We found that increasing infiltration of Neutrophils, T cells regulatory, CD4 T memory activated cells, NK cells activated, Mast cells activated as well as reducing infiltration of Eosinophils, Macrophages M0 and CD8 T cells may be associated with cirrhosis pathogenesis. Neutrophils are usually recruited to the liver at the early stage of liver injury to clear apoptosis hepatocytes[19] and it releases cell-free DNA with strong pro-inflammatory effect[20]. Cirrhosis mouse model showed the development of liver fibrosis was alleviated by deletion or ablation of neutrophils of neutrophil chemokines [21, 22]. In the fibrosing process, injection-induced inflammation and then triggered macrophages to gather in the liver, which then induces the activation of hepatic stellate cells (HSCs) by producing cytokines and chemokines[23]. In turn, macrophages can promote myofibroblast apoptosis by expressing MMP9 and TRAIL[24], and enhance epithelial-mesenchymal transformation (ECM) degradation to alleviate fibrosis in rodent models[24, 25]. Activated liver-associated NK cells may be antifibrogenic by killing HSCs and releasing IFNγ[26]. However, CD4+T lymphocytes inhibit NK cells through interaction with NK cells and activated hematopoietic stem cells, which is conducive to the favor of hematopoietic stem cells[27]. In addition, other studies showed that CD8+T cell ablation can accelerate hepatocellular carcinoma[28]. indicating that IRGs in cirrhosis are involved in the immune and inflammatory processes of the disease.

Subsequently, a four potential hub DEGs (*ACTB, TAGLN, VIM* and *SOX9*) were attained via the five methods of Cytoscape and judged to be the core genes for the immune and inflammatory responses, based on the results of GO and KEGG analysis. Beta-actin (*ACTB*) is believed in constitutive housekeeping gene[29] and it as an ample and highly conserved cytoskeleton structural protein, it is generally dispersed in all eukaryotic cells and plays vital roles in cell division, cell migration, immune response and gene expression[30-32]. Growing evidence shows that 3'-UTR of *ACTB* was closely corelated with the development of liver cancer[33]. Although previously studies had shown that *ACTB* levels were not correlated with cirrhosis, recent studies had shown that *ACTB* were involved in circulatory inflammation /angiogenesis index[34]. Therefore, whether the disorder of *ACTB*-dependent immune response can facilitate leukocyte recruitment and support inflammation in cirrhosis needs further study.

TAGLN is an actin crosslinking protein expressed in fibroblasts, endothelial cells, and immune cells in many different cell types and interacts with calcECium to regulate contraction located in the cytoplasm[35, 36]. Overexpression of *TAGLN* protein had been observed in human hepatocellular carcinoma patients[37]. In addition, it was found in mouse model studies that vascular endothelial growth factor A can simultaneously activate *TAGLN* promoter and endothelial cell elongation, and it is speculated that *TAGLN* may be A regulatory factor of angiogenesis[38-40]. Hence, we hypothesized that *TAGLN* may have an effect on cirrhosis through matrix remodeling and migration, differentiation, invasion of cell.

Vimentin (*VIM*) belongs to the family of intermediate filaments, which are specifically found in connective tissues[41]. *VIM* gene encodes Vimentin, which not only plays a vital role in preserving cell morphology and stabilizing cytoskeleton interactions, but also plays a significant role in cell migration, inflammation, signal transduction and other biological processes[42]. Recently, *VIM* as one of SOX9 targets amenable to adjust the advance of liver fibrosis[43], which was in line with our present study.

Previously, researches had shown that ectopic expression of gender-determining transcription factor Y-box 9 (*SOX9*) take charge of type 1 collagen production in activated hematopoietic stem cells[44]. A clinical biopsy study of cirrhosis found that *SOX9* expression levels in chronic liver disease related to the

seriousness of fibrosis and precisely predicted the cirrhosis progression[45]. Further study identified that extracellular protein epimorphin regulate the excessive ECM environment generated by activated HSCs, through down-regulation of pro-fibrotic *SOX9,* up to a point[46]. Recently, a molecular study proved that HBV activates *SOX9* expression via inducing increased *SOX9* promoter activity. Interestingly, in turn, *SOX9* inhibits HBV replication by straightly binding to EnhII/Cp by inhibiting EnhII/Cp activation[47]. These researches display the hub role of *SOX9* as a regulator of fibrotic ECM components in the progression of liver fibrosis[48, 49], which was consistent with our present study.

Subsequently, we further investigated the association between *ACTB, TAGLN, VIM, SOX9* and immune infiltration. We found *ACTB* was positively correlated with Type 17 T helper cell, activated B cell, Macrophage, Mast cell, Effector memory CD8 T cell and negatively correlated with CD56dim natural killer cell, Type 1and 2 T helper cell. *TAGLN* was positively associated with Central memory CD4 T cell, Monocyte, and correlated negatively with Macrophage, Eosinophil, Regulatory T cell, Natural killer T cell, Type 17 T helper cell. *VIM* was positively related to activated B cell, Mast cell, Effector memory CD8 T cell, and correlated negatively with helper cell of Type 1 T, T helper cell of Type 2. *SOX9* was positively correlated with T helper cell of Type 17, activated B cell, mast cell, Effector memory CD8 T cell, and correlated negatively with T helper cell of Type 1, T helper cell of Type 2, CD56dim natural killer cell.

Finally, the mechanism incidence and progress of cirrhosis by which four hub DEIRGs effects, bioinformatics tools were used to detect KEGG pathway and their associated genes. Our study analysis revealed that variations in greatest genes with strong associations with *ACTB* expression mainly affect pathways associated with the internalization and formation of the phagosomes.

According to above results, *ACTB, TAGLN, VIM* and *SOX9* appear to play hub roles in cirrhosis via the regulating immune infiltration.

5. Conclusion

In summary, we found *ACTB, TAGLN, VIM* and *SOX9* may be key biomarkers of liver cirrhosis. Moreover, correlations between ten hub DEGs and immune cells may play a critical role in the pathogenesis of cirrhosis.

Limitation

Several limitations should be highlighted in our study. First, the results are just a microarray and immune-related analysis that based on gene expression value and immune database. Besides, although the results of cirrhosis-related key DEGs and immune cells are enlightening, we at present do not exactly understand how those genes contribute to the cirrhosis. Therefore, further experiments are needed for verification of the biological function of these genes.

Abbreviations

DEGs: differentially expressed genes

GO: Gene ontology

KEGG: Kyoto Encyclopedia of Genes and Genomes

PPI: protein-protein interaction

Declarations

Acknowledgments

None.

Authors' contributions

Conceptualized and designed the study: TY D and, Y S Z; Data analysis: TY D; Result interpretation: TY D; Wrote the paper: TY D. All the authors have read and approved the final manuscript.

Funding

This work was supported by the General project of Social Development of Science and Technology Department of Jiangsu Province [No. BE2016613].

Data Availability Statement

All the data were acquired from the Gene Expression Omnibus (GEO) database.

Ethics approval and consent to participate

Not applicable.

Consent for publication

Not applicable.

Competing interests

The authors declare that they have no competing interests.

References

[1] Lozano R, Naghavi M, Foreman K, et al. Global and regional mortality from 235 causes of death for 20 age groups in 1990 and 2010: a systematic analysis for the Global Burden of Disease Study 2010. Lancet. 2012. 380(9859): 2095-128.

[2] Blachier M, Leleu H, Peck-Radosavljevic M, Valla DC, Roudot-Thoraval F. The burden of liver disease in Europe: a review of available epidemiological data. J Hepatol. 2013. 58(3): 593-608.

[3] Hoyert DL, Xu J. Deaths: preliminary data for 2011. Natl Vital Stat Rep. 2012. 61(6): 1-51.

[4] Keerthikumar S. An Introduction to Proteome Bioinformatics. Methods Mol Biol. 2017. 1549: 1-3.

[5] Oliver GR, Hart SN, Klee EW. Bioinformatics for clinical next generation sequencing. Clin Chem. 2015. 61(1): 124-35.

[6] Charoentong P, Finotello F, Angelova M, et al. Pan-cancer Immunogenomic Analyses Reveal Genotype-Immunophenotype Relationships and Predictors of Response to Checkpoint Blockade. Cell Rep. 2017. 18(1): 248-262.

[7] Barrett T, Wilhite SE, Ledoux P, et al. NCBI GEO: archive for functional genomics data sets–update. Nucleic Acids Res. 2013. 41(Database issue): D991-5.

[8] Davis S, Meltzer PS. GEOquery: a bridge between the Gene Expression Omnibus (GEO) and BioConductor. Bioinformatics. 2007. 23(14): 1846-7.

[9] Shade A, Handelsman J. Beyond the Venn diagram: the hunt for a core microbiome. Environ Microbiol. 2012. 14(1): 4-12.

[10] Kanehisa M, Goto S. KEGG: kyoto encyclopedia of genes and genomes. *Nucleic Acids Res*. 2000;28:27-30.

[11] Chen B, Khodadoust MS, Liu CL, Newman AM, Alizadeh AA. Profiling Tumor Infiltrating Immune Cells with CIBERSORT. Methods Mol Biol. 2018. 1711: 243-259.

[12] Gu Z, Eils R, Schlesner M. Complex heatmaps reveal patterns and correlations in multidimensional genomic data. Bioinformatics. 2016. 32(18): 2847-9.

[13] Li J, Zou B, Yeo YH, Feng Y, Xie X, Lee DH, Fujii H, Wu Y, Kam LY, Ji F, Li X, Chien N, Wei M, Ogawa E, Zhao C, Wu X, Stave CD, Henry L, Barnett S, Takahashi H, Furusyo N, Eguchi Y, Hsu YC, Lee TY, Ren W, Qin C, Jun DW, Toyoda H, Wong VW, Cheung R, Zhu Q, Nguyen MH. Prevalence, incidence, and outcome of non-alcoholic fatty liver disease in Asia, 1999-2019: a systematic review and meta-analysis. *Lancet Gastroenterol Hepatol*. 2019;4:389-398.

[14] Tsochatzis EA, Bosch J, Burroughs AK. Liver cirrhosis. *Lancet*. 2014;383:1749-1761.

[15] Ge PS, Runyon BA. Treatment of Patients with Cirrhosis. N Engl J Med. 2016. 375(8): 767-77.

[16] Kisseleva T, Brenner D. Molecular and cellular mechanisms of liver fibrosis and its regression. Nat Rev Gastroenterol Hepatol. 2021. 18(3): 151-166.

[17] Parola M, Pinzani M. Liver fibrosis: Pathophysiology, pathogenetic targets and clinical issues. Mol Aspects Med. 2019. 65: 37-55.

[18] Kisseleva T, Uchinami H, Feirt N, et al. Bone marrow-derived fibrocytes participate in pathogenesis of liver fibrosis. J Hepatol. 2006. 45(3): 429-38.

[19] Mridha AR, Wree A, Robertson A, Yeh MM, Johnson CD, Van Rooyen DM, Haczeyni F, Teoh NC, Savard C, Ioannou GN, Masters SL, Schroder K, Cooper MA, Feldstein AE, Farrell GC. NLRP3 inflammasome blockade reduces liver inflammation and fibrosis in experimental NASH in mice. *J Hepatol*. 2017;66:1037-1046.

[20] Meier A, Chien J, Hobohm L, Patras KA, Nizet V, Corriden R. Inhibition of Human Neutrophil Extracellular Trap (NET) Production by Propofol and Lipid Emulsion. *Front Pharmacol*. 2019;10:323.

[21] Saijou E, Enomoto Y, Matsuda M, Yuet-Yin Kok C, Akira S, Tanaka M, Miyajima A. Neutrophils alleviate fibrosis in the CCl4-induced mouse chronic liver injury model. *Hepatol Commun*. 2018;2:703-717.

[22] Gehrke N, Nagel M, Straub BK, W?rns MA, Schuchmann M, Galle PR, Schattenberg JM. Loss of cellular FLICE-inhibitory protein promotes acute cholestatic liver injury and inflammation from bile duct ligation. *Am J Physiol Gastrointest Liver Physiol*. 2018;314:G319-G333.

[23] Iredale JP. Models of liver fibrosis: exploring the dynamic nature of inflammation and repair in a solid organ. *J Clin Invest*. 2007;117:539-548.

[24] Ramachandran P, Pellicoro A, Vernon MA, Boulter L, Aucott RL, Ali A, Hartland SN, Snowdon VK, Cappon A, Gordon-Walker TT, Williams MJ, Dunbar DR, Manning JR, van Rooijen N, Fallowfield JA, Forbes SJ, Iredale JP. Differential Ly-6C expression identifies the recruited macrophage phenotype, which orchestrates the regression of murine liver fibrosis. *Proc Natl Acad Sci U S A*. 2012;109:E3186-3195.

[25] Popov Y, Sverdlov DY, Bhaskar KR, Sharma AK, Millonig G, Patsenker E, Krahenbuhl S, Krahenbuhl L, Schuppan D. Macrophage-mediated phagocytosis of apoptotic cholangiocytes contributes to reversal of experimental biliary fibrosis. *Am J Physiol Gastrointest Liver Physiol*. 2010;298:G323-334.

[26] Jeong WI, Park O, Radaeva S, Gao B. STAT1 inhibits liver fibrosis in mice by inhibiting stellate cell proliferation and stimulating NK cell cytotoxicity. *Hepatology*. 2006;44:1441-1451.

[27] Langhans B, Alwan AW, Kr?mer B, Gl?ssner A, Lutz P, Strassburg CP, Nattermann J, Spengler U. Regulatory CD4+ T cells modulate the interaction between NK cells and hepatic stellate cells by acting on either cell type. *J Hepatol*. 2015;62:398-404.

[28] Shalapour S, Lin XJ, Bastian IN, Brain J, Burt AD, Aksenov AA, Vrbanac AF, Li W, Perkins A, Matsutani T, Zhong Z, Dhar D, Navas-Molina JA, Xu J, Loomba R, Downes M, Yu RT, Evans RM, Dorrestein PC, Knight R, Benner C, Anstee QM, Karin M. Inflammation-induced IgA+ cells dismantle anti-liver cancer immunity. *Nature*. 2017;551:340-345.

[29] Popow A, Nowak D, Malicka-B?aszkiewicz M. Actin cytoskeleton and beta-actin expression in correlation with higher invasiveness of selected hepatoma Morris 5123 cells. *J Physiol Pharmacol*. 2006;57 Suppl 7:111-123.

[30] Ruan W, Lai M. Actin, a reliable marker of internal control. *Clin Chim Acta*. 2007;385:1-5.

[31] Bunnell TM, Burbach BJ, Shimizu Y, Ervasti JM. ??-Actin specifically controls cell growth, migration, and the G-actin pool. *Mol Biol Cell*. 2011;22:4047-4058.

[32] Drazic A, Aksnes H, Marie M, Boczkowska M, Varland S, Timmerman E, Foyn H, Glomnes N, Rebowski G, Impens F, Gevaert K, Dominguez R, Arnesen T. NAA80 is actin's N-terminal acetyltransferase and regulates cytoskeleton assembly and cell motility. *Proc Natl Acad Sci U S A*. 2018;115:4399-4404.

[33] Li Y, Ma H, Shi C, Feng F, Yang L. Mutant ACTB mRNA 3'-UTR promotes hepatocellular carcinoma development by regulating miR-1 and miR-29a. *Cell Signal*. 2020;67:109479.

[34] Bednarz-Misa I, Neubauer K, Zacharska E, Kapturkiewicz B, Krzystek-Korpacka M. Whole blood ACTB, B2M and GAPDH expression reflects activity of inflammatory bowel disease, advancement of colorectal cancer, and correlates with circulating inflammatory and angiogenic factors: Relevance for real-time quantitative PCR. *Adv Clin Exp Med*. 2020;29:547-556.

[35] Assinder SJ, Stanton JA, Prasad PD. Transgelin: an actin-binding protein and tumour suppressor. *Int J Biochem Cell Biol*. 2009;41:482-486.

[36] Dvorakova M, Nenutil R, Bouchal P. Transgelins, cytoskeletal proteins implicated in different aspects of cancer development. *Expert Rev Proteomics*. 2014;11:149-165.

[37] Rho JH, Roehrl MH, Wang JY. Tissue proteomics reveals differential and compartment-specific expression of the homologs transgelin and transgelin-2 in lung adenocarcinoma and its stroma. *J Proteome Res*. 2009;8:5610-5618.

[38] Shapland C, Hsuan JJ, Totty NF, Lawson D. Purification and properties of transgelin: a transformation and shape change sensitive actin-gelling protein. *J Cell Biol*. 1993;121:1065-1073.

[39] Tsuji-Tamura K, Ogawa M. Inhibition of the PI3K-Akt and mTORC1 signaling pathways promotes the elongation of vascular endothelial cells. *J Cell Sci*. 2016;129:1165-1178.

[40] Tsuji-Tamura K, Morino-Koga S, Suzuki S, Ogawa M. The canonical smooth muscle cell marker TAGLN is present in endothelial cells and is involved in angiogenesis. *J Cell Sci*. 2021;134.

[41] Fuchs E, Weber K. Intermediate filaments: structure, dynamics, function, and disease. *Annu Rev Biochem*. 1994;63:345-382.

[42] Jung S, Yi L, Kim J, Jeong D, Oh T, Kim CH, Kim CJ, Shin J, An S, Lee MS. The role of vimentin as a methylation biomarker for early diagnosis of cervical cancer. *Mol Cells*. 2011;31:405-411.

[43] Athwal VS, Pritchett J, Martin K, Llewellyn J, Scott J, Harvey E, Zaitoun AM, Mullan AF, Zeef L, Friedman SL, Irving WL, Hanley NA, Guha IN, Piper Hanley K. SOX9 regulated matrix proteins are increased in patients serum and correlate with severity of liver fibrosis. *Sci Rep*. 2018;8:17905.

[44] Hanley KP, Oakley F, Sugden S, Wilson DI, Mann DA, Hanley NA. Ectopic SOX9 mediates extracellular matrix deposition characteristic of organ fibrosis. *J Biol Chem*. 2008;283:14063-14071.

[45] Athwal VS, Pritchett J, Llewellyn J, Martin K, Camacho E, Raza SM, Phythian-Adams A, Birchall LJ, Mullan AF, Su K, Pearmain L, Dolman G, Zaitoun AM, Friedman SL, MacDonald A, Irving WL, Guha IN, Hanley NA, Piper Hanley K. SOX9 predicts progression toward cirrhosis in patients while its loss protects against liver fibrosis. *EMBO Mol Med*. 2017;9:1696-1710.

[46] Pritchett J, Athwal VS, Harvey E, Martin K, Llewellyn J, Ireland P, Nicolaides A, Humphries MJ, Bobola N, Hanley NA, Piper Hanley K. Epimorphin alters the inhibitory effects of SOX9 on Mmp13 in activated hepatic stellate cells. *PLoS One*. 2014;9:e100091.

[47] Yang H, Zhou Y, Mo J, Xiang Q, Qin M, Liu W, Shang J, Yang Q, Xu W, Yang G, Tan Q, Wu K, Liu Y, Wu J. SOX9 represses hepatitis B virus replication through binding to HBV EnhII/Cp and inhibiting the promoter activity. *Antiviral Res*. 2020;177:104761.

[48] Zhao L, Li T, Wang Y, Pan Y, Ning H, Hui X, Xie H, Wang J, Han Y, Liu Z, Fan D. Elevated plasma osteopontin level is predictive of cirrhosis in patients with hepatitis B infection. *Int J Clin Pract*. 2008;62:1056-1062.

[49] Huang W, Zhu G, Huang M, Lou G, Liu Y, Wang S. Plasma osteopontin concentration correlates with the severity of hepatic fibrosis and inflammation in HCV-infected subjects. *Clin Chim Acta*. 2010;411:675-678.

Tables

Table 1 Differentially expressed genes (DEGs) name

RORA	SLITRK3	NUBPL	VMO1	ACSL5	NCOR1	AMHR2	NAMPT	HSD17B14	PEG3	KCNAB1	MT
SGK3	PALM2	UBR3	HIVEP1	WEE1	PPARGC1A	NFKBIA	SUCNR1	MT1H	IGFALS	CLEC1B	TP
PSME4	FCN2	GCNT2	SDHC	GFOD2	AOX1	MARCO	TTC36	AADAT	THOP1	ANKRD35	RA
NR5A2	ZCCHC6	KBTBD11	LRRFIP2	DNAJC12	SLC1A1	SLC13A5	GCAT	HEY2	CACNA1H	SOCS2	US
ITCH	PPP3R1	DMD	CLEC4G	KCNN2	SLC16A10	TSPAN7	IRS2	COBLL1	CNDP1	MAN1C1	ER
KLHL15	CLEC4M	RALGPS2	PACSIN3	LONP2	JUND	FNIP2	MAT1A	PON1	AGL	MBNL2	GS
CETP	STYX	LYVE1	CNST	DNASE1L3	AVPR1A	ZYG11B	MT1E	FAM151A	SMOC1	TAT	AK
GPC6	OSBPL8	FAM46A	CFL2	UPP1	TRIB1	ABCC9	FCN3	IL1RN	SGMS2	FOLH1	C7
RBMS1	STRN3	RAD21	HPR	STAB2	GALK1	RCAN1	RNF125	PCDH20	CCL3	ST3GAL6	LG
CCL23	IFT88	EGFLAM	DNAJB9	MT1M	CYP2C19	DCAF11	GADD45G	SLC39A14	GCH1	SYBU	AN
ZRANB1	FITM1	C5	SLC38A2	ABCA1	ADRB2	MT1X	PCOLCE2	EGFR	GFRA1	CFHR3	FA
MBNL3	FAM134B	DEXI	RNF19A	MT1F	RELN	SAMD4A	LILRB5	ITLN1	OIT3	GLUD1	SL
GMNN	CD151	CLDN10	TBC1D10C	FXYD2	CCDC3	CFTR	SCTR	BACE2	PRICKLE1	CCL19	SP
STMN2	VSIG2	RNASE1	LAMA2	ACTB	SPINT2	AEBP1	SEL1L3	FBLN2	S100A4	SCRN1	NK
EPHA3	GPC3	RTP4	CD24	PDGFRA	SSPN	CYBRD1	DMKN	COL6A2	CLDN7	CCDC146	CY
SH3YL1	ZBED5	ST14	LBH	S100A10	MOXD1	ENPP5	TMPRSS3	CDH6	SYT13	SUSD2	MM
MICALL2	SDCBP2	LRRC1	APOL3	TRIM22	ADAMTSL2	COL15A1	VIM	TESC	IGSF3	KRT7	GP
BCL11A	AKR1B15	AQP1	SELM	GLS	WDR13	CLIC6	LAMC3	ZNF827	CHST9	C1orf106	SL
GOLM1	ID3	SLC38A1	KIAA1522	DEFB1	SOX9	LGALS3	FAP	PECAM1	IFI16	S100A6	GA
CLDN11	APBB3	FAM129B	SFRP5	RCAN2	PLCXD3	SPON2	LTBP4	PDGFRB	FAT1	CXCL6	HK
PAPLN	TSPAN8	ANXA13	FAM150B	DTNA	KRT23	C1orf198	SLFN11	ZMAT3	CITED4	TMEM200A	CR
CD48	SPATA18	DKK3	CCL21	PLAT	MPV17	RHOC	ANTXR1	TYMS	SREBF1	COL1A2	SE
ACTG1	ZNF83	NR2F2	HLA-A	ATP8B2	SNRPN	MFAP4	SNAP25	TPM1	ITGB5	CSNK1G2	EF

Table 2 KEGG pathway enrichment analysis of ACTB, PECAM1, COL1A2, PDGFRA and PDGFRB-related genes

ID	Gene set name	Gene-Ratio	Bg-Ratio	p-value	p-adjust	q-value	Gene-ID	Count
hsa04145	Phagosome	19/286	156/5894	0.000173	0.010688	0.009061	HLAF/CLEC4M/HLA-DQB1/ACTG1/RAC1/HLA-G/HLA-A/ACTB/HLA-DOB/MARCO/TUBA1A/CORO1A/HLA-DRA/ITGB5/HLA-DPB1/TUBB2A/TUBA1C/COLEC11/FCGR2A	19

Figures

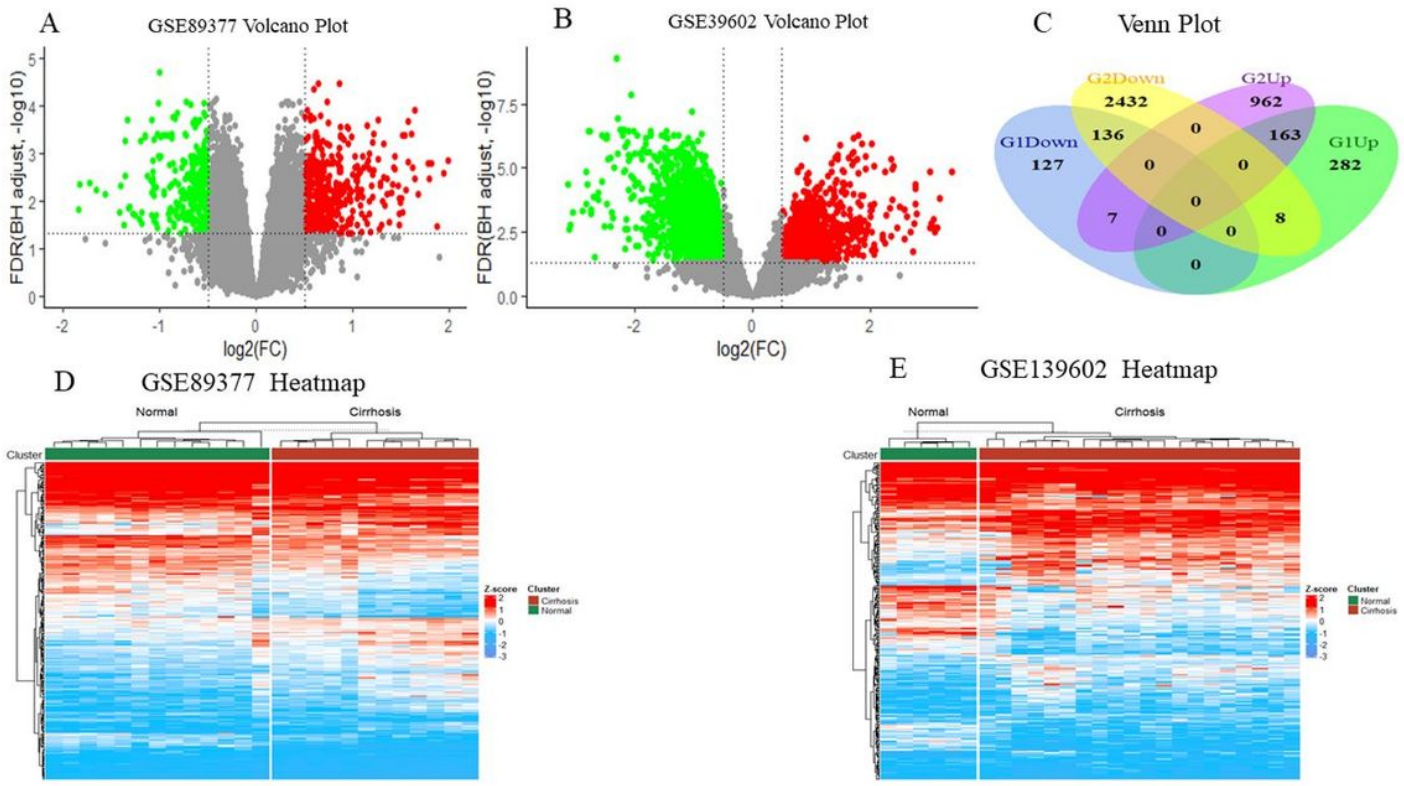

Figure 1

Volcano plots (A) and the Volcano plots (B) of all up-and down-regulated genes to show the DEGs data between normal liver and cirrhosis samples from GSE89377 and GSE39602 respectively. Red, greater expression. Green, less expressive. Venn Diagram (C) of overlapping two microarray datasets DEGs to show the intersection of upward and downward revisions of the two sets of data. The intersection of G1Down and G2Down was represented both upregulated in two data. The intersection of G1Up and G2Up was represented both downregulated in two data. An absolute log2 FC > 0.5 and an adjusted *P* value of < 0.05 cutoff was used to define differentially expressed mRNAs in cirrhosis.

DEGs: Differentially expressed genes; G1Up: upregulated genes in GSE89377; G2Up: upregulated genes in GSE39602; G1Down: downregulated genes in GSE89377; G2Down: downregulated genes in GSE39602. Heatmap (D) of the showing the genes expression changes between normal liver and cirrhosis of GSE89377. Heatmap (E) of the showing the genes expression change between normal liver and cirrhosis of GSE39602.

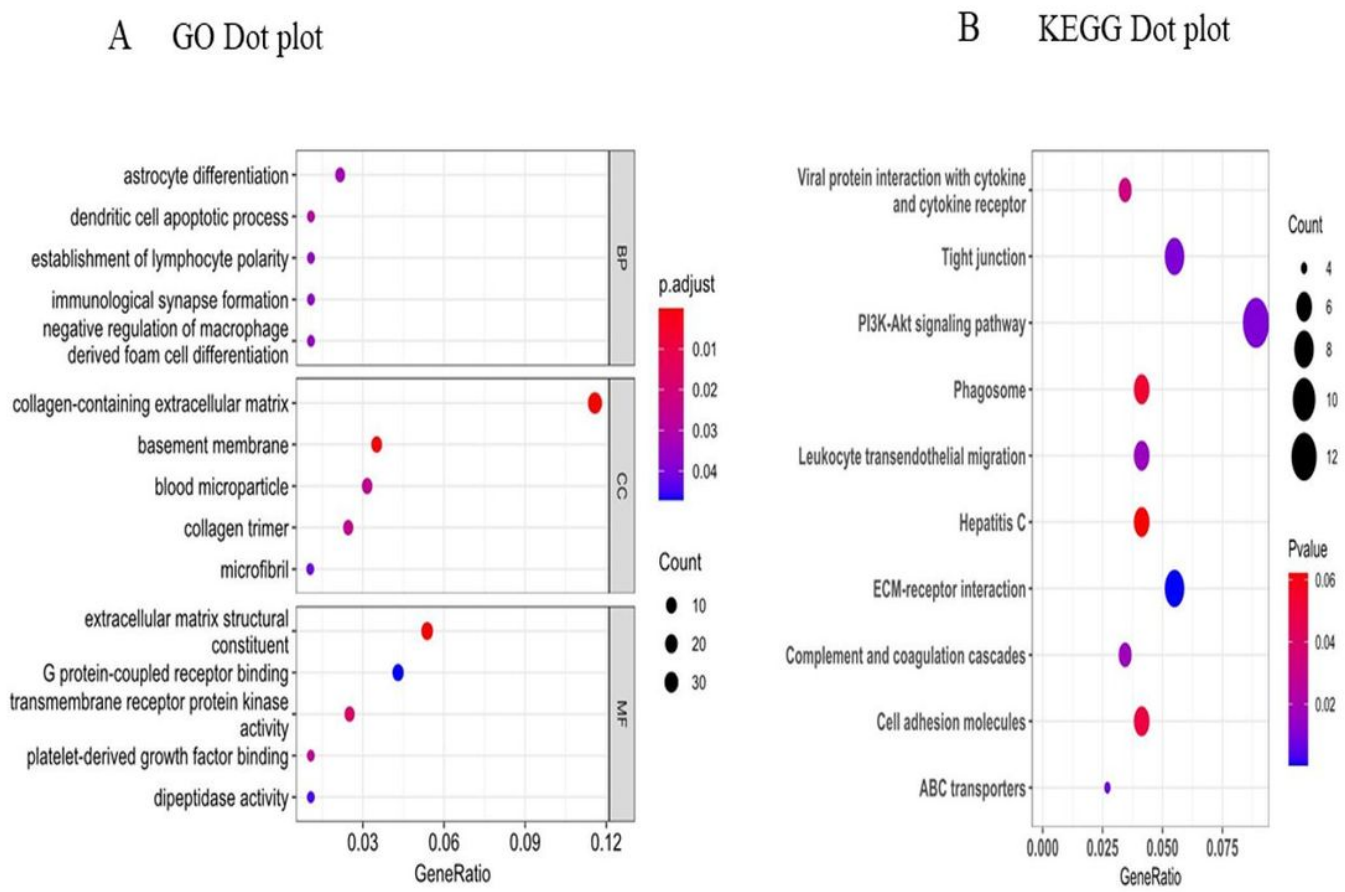

Figure 2

Enrichment analysis on cirrhosis-related DEGs.

(A) GO analysis and (B) KEGG pathway enrichment analysis. GO: Gene Ontology;

KEGG: Kyoto Encyclopedia of Genes and Genomes.

DEGs: differentially expressed genes

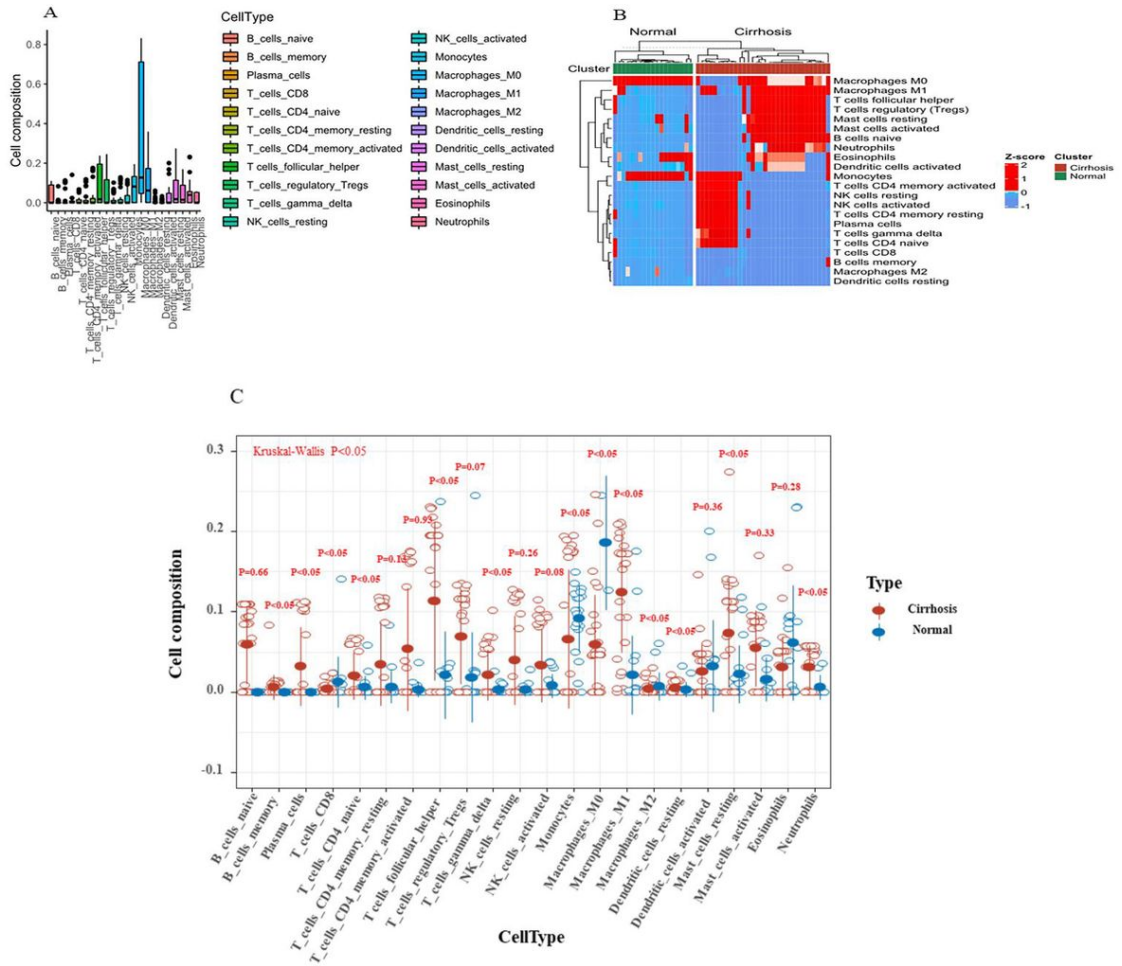

Figure 3

Boxplot (A) of the showing the proportion of 22 immune cells in all samples. Heatmap (B) of the showing the 22immune cells expression change between normal liver and cirrhosis of two databases. Strip chart (C) of showing the expression levels of 22 immune cells in normal liver tissue and cirrhosis. Red: cirrhosis; Blue: normal.

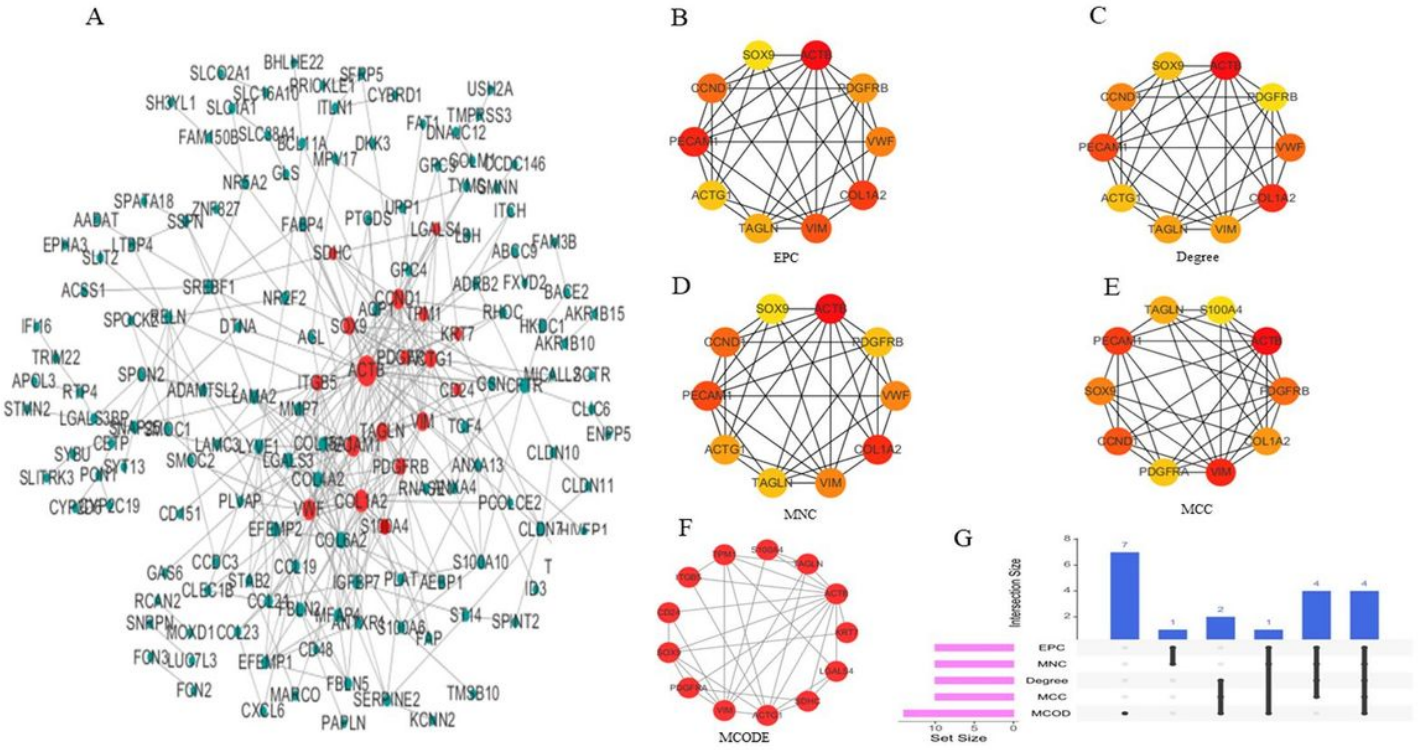

Figure 4

PPI network construction and identification of hub DEGs.

(A) The protein-protein interaction network of differentially co-expressed cirrhosis-related genes. (B) The top 10 hub DEGS extracted by EPC have the highest connectivity (color depth for ranking of hub DEGs). (C) Top 10 hub DEGs be identified by Degree with the highest connectivity (color depth for ranking of hub DEGs). (D) Top 10 hub DEGs be identified by MNC with the highest connectivity (color depth for ranking of hub DEGs). (E) Top 10 hub DEGs be identified by MCC with the highest connectivity (color depth for ranking of hub DEGs). (F) Top 10 hub DEGs be identified by MCODE with the highest connectivity (color depth for ranking of hub DEGs). (G) The Upset diagram shows the intersection of the top ten HUB genes obtained by the above five methods (Pink bar represents the five methods, blue bar represents the intersect genes).

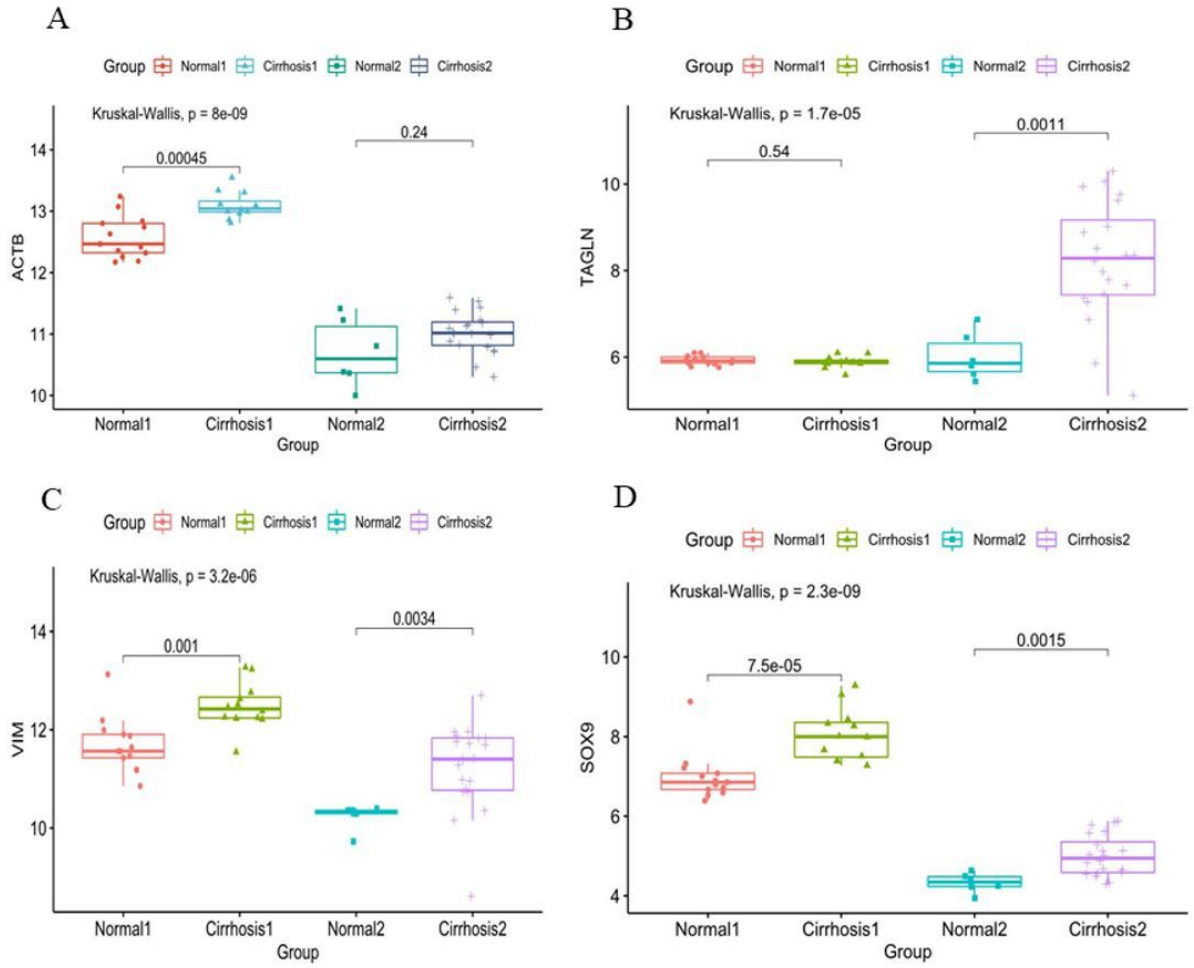

Figure 5

Expression analysis of ten hub DEGs in two data groups normal group and cirrhosis group.

(A) The expression pattern of *ACTB* in normal sample and cirrhosis sample among GSE89377, GSE139602. (B) The expression pattern of *TAGLN* in normal sample and cirrhosis sample among GSE89377, GSE139602. (C) The expression pattern of *VIM* in normal sample and cirrhosis sample among GSE89377, GSE139602. (D) The expression pattern of *SOX9* in normal sample and cirrhosis sample among GSE89377, GSE139602.

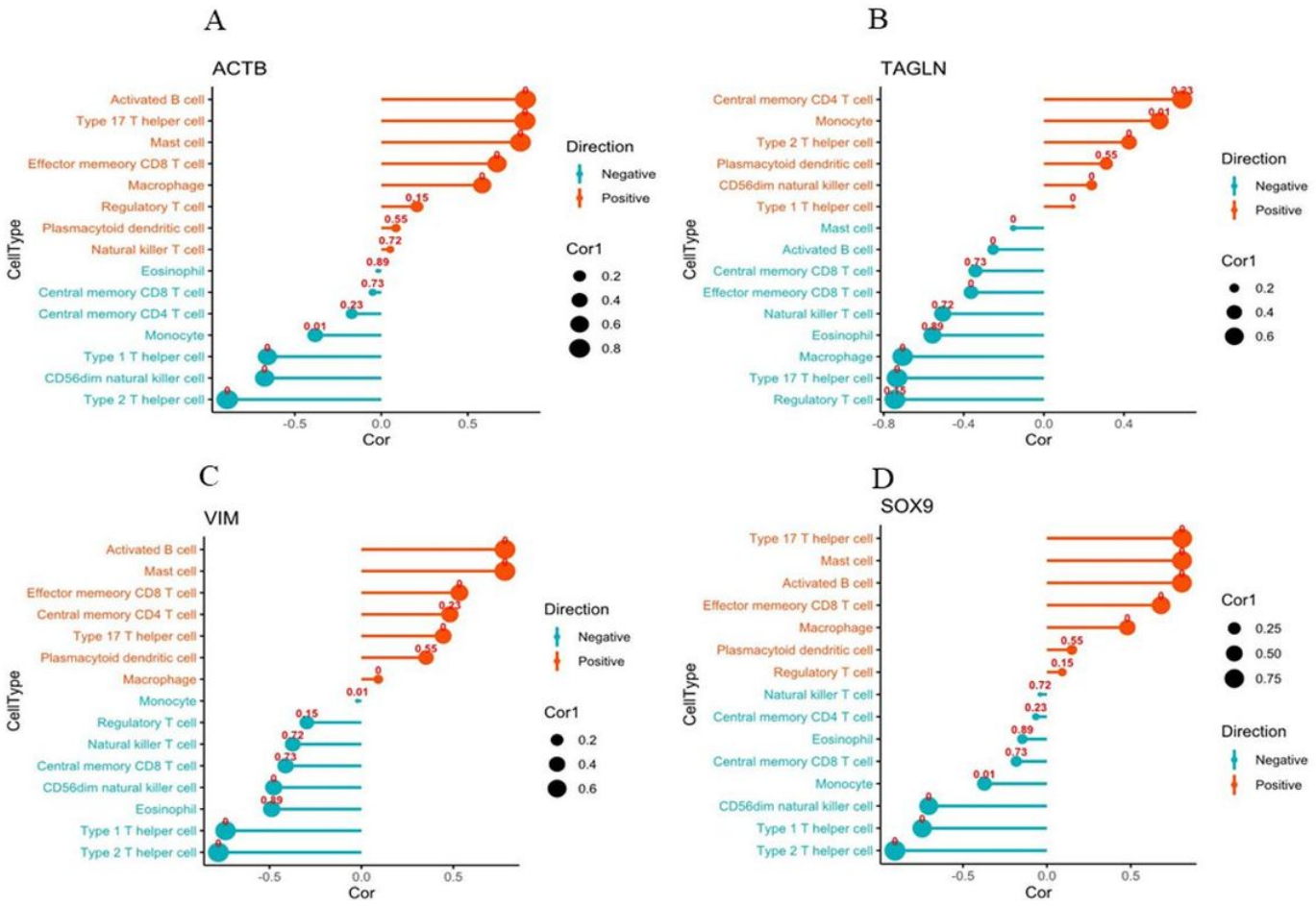

Figure 6

Correlations between ten hub DEGs and infiltrating immune cells.

(A)Correlation between *ACTB* and infiltrating immune cells. (B) Correlation between *TAGLN* and infiltrating immune cells. (C) Correlation between *VIM* and infiltrating immune cells. (D) Correlation between *SOX9* and infiltrating immune cells. Size of the dots represents the strength of the correlation between key immune related genes and immune cells; the larger (or smaller) the dots, the stronger (or weaker) the correlation. Color of the dots represents the negative or positive correlation; the green color: negative correlation, the red color: positive correlation. The number on the dots-upside represents the P value; P<0.05 and absolute value (Cor) > 0.5 were considered statistically significant. Cor: correlation;

A hsa04145(ACTB)Pathway

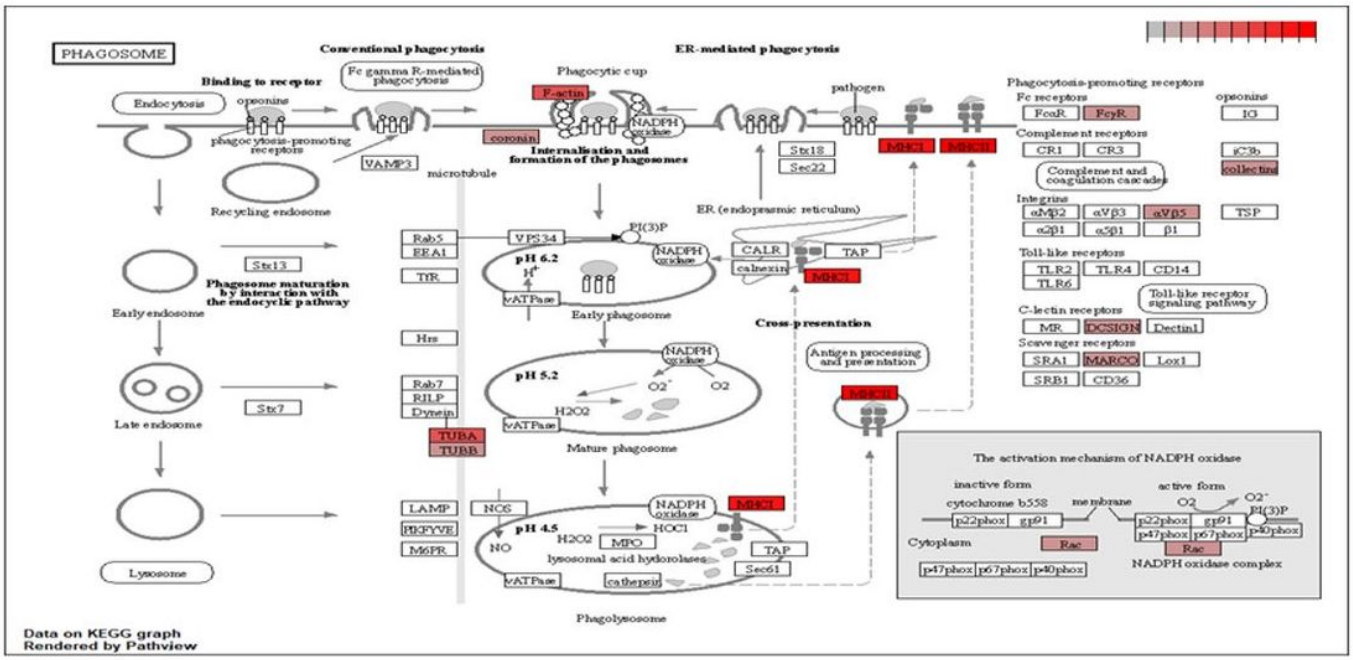

Figure 7

ACTB-associated genes related position in KEGG pathway.

Positional relationships of *ACTB*-associated genes in the phagosome. *ACTB*-related genes in phagosome pathway are brought into the website related to the KEGG pathway to generate a road map, and the relevant positions of the corresponding genes in the pathway are marked with red circles according to the degree of impact.

Supplementary Files

This is a list of supplementary files associated with this preprint. Click to download.

- GSE89377seriesmatrix.xls
- GSE139602seriesmatrix.xls
- LM22.xls